

# Radio Observations of 4079 Quasars

Otto B. Bischof

Physics Department, University of California, Davis, CA 95616

and

Institute of Geophysics & Planetary Physics, LLNL, Livermore, CA 94550

obischof@igpp.llnl.gov

Robert H. Becker

Physics Department, University of California, Davis, CA 95616

and

Institute of Geophysics & Planetary Physics, LLNL, Livermore, CA 94550

bob@igpp.llnl.gov

Version: 10 Feb 1997

Received \_\_\_\_\_; accepted \_\_\_\_\_

## ABSTRACT

Using the NVSS radio catalog, we have searched for radio emission from 4079 quasars taken from the 1996 version of the Veron-Cetty and Veron (1996) quasar catalog. The comparison resulted in the positive detection of radio emission from 799 quasars. Of these, 168 are new radio detections. Examination of the radio luminosities shows a dramatic increase in the fraction of radio-loud quasars from the current epoch to  $z=0.5$  and a gradual decline beyond  $z=1.0$ . Inspection of the radio-loud fraction as a function of  $M_B$  shows little dependence fainter than  $M_B=-29.5$ .

## 1. Introduction

Although quasars were originally discovered as a result of their radio emission, it is now clear that a majority of quasars are 'radio-quiet'. It is common to classify quasars as radio-loud or radio-quiet either based on their radio luminosity or on the ratio of their radio to optical luminosities. The latter ratio is known to span a range of 5 orders of magnitude. To date there is no generally accepted explanation for the difference between radio-loud and radio-quiet quasars.

One avenue of research has been to search for correlations between the fraction of radio-loud quasars ( $F_{\text{RLQ}}$ ) with other observables. It is still an open question whether radio-loud and radio-quiet quasars are two distinct classes of objects or represent a continuous distribution of radio to optical power. Previous studies have attempted to define unbiased samples of quasars to address the nature of radio-loud quasars. These samples have been drawn from optically and x-ray selected quasar surveys. Their main drawback has been the relatively small size of the samples. In contrast, this study emphasizes quantity at the risk of introducing unrecognized biases. That is to say, in this work we will examine the radio emission from all known quasars over a large region of sky independent of how the individual quasars were discovered. This has one key advantage, a very large sample, which optimistically may compensate for the diversity of the sample.

In a recent study, Hooper *et al.* (1996) presented a sample of 61 VLA radio detections among 359 optically selected quasars from the Large Bright Quasar Survey (LBQS) (Hewett *et al.* 1995). They computed  $F_{\text{RLQ}}$  as a function of redshift and absolute magnitude and found that it was only weakly dependent on either quantity. In this paper we present a similar study for a much larger sample of quasars. Using the National Radio Astronomy Observatory Very Large Array Sky Survey (NVSS) (Condon 1995), we have searched for radio emission from 4079 quasars (47 % of the quasars currently known) in the latest edition of the Veron catalog (Veron-Cetty and Veron 1996, hereafter VV) which lie within the area of sky covered by the NVSS.

## 2. Radio/Optical Comparisons

This exercise is possible because of new radio surveys which are becoming available. In particular, the VLA is currently being used to survey 75 % of the sky at 1400 MHz. The survey, formally known as the NVSS, has an angular resolution of  $\sim 45$  arcsec and a 5 sigma sensitivity of  $\sim 2.4$  mJy. To date, data for approximately one third of the eventual sky coverage has been released.

Our methodology is straightforward. We compare the positions of quasars in VV to the positions of radio sources in the NVSS catalog and calculate the separation between each quasar and the nearest radio source. We estimate the chance coincidence rate by repeating the experiment with a false quasar catalog generated by shifting the positions in VV by 1 degree. (Note that the chance coincidence rate is in agreement with expectations for a random distribution.) The spatial distribution of quasars that fall within the NVSS survey as of May 1, 1996 is shown in Figure 1. The obvious nonuniform distribution of quasars on the sky is a direct result of inhomogeneous sky coverage of surveys. In Figure 2, we show a histogram of the angular separations between the known quasars and the nearest radio source both for VV as well as the false quasar catalog. We conclude that matches within 10 arcsec are 98 % real while matches beyond 35 arcsec are almost totally chance coincidences. (Note that 10 arcsec is approximately equal to the radius of the 90 % confidence error circle for a 2.4mJy source). The 149 matches between 10-35 arcsec are a mixture of real (60 %) and chance (40 %) coincidences and will not be included in this study even though they constitute 10 % of the real matches. In summary, we find 799 radio detections of quasars, including 168 new detections which are listed in Table 1, 3280 nondetections for which we assign an upper limit of 2.4 mJy, and 149 ambiguous matches which we discard. There has been no attempt to identify which of the quasars were originally discovered as a result of their radio emission.

### 3. Results

In Figure 3, we show a histogram of the 1400 MHz flux densities up to 2 Jy of the 799 quasars with counterparts in the NVSS. The shaded histogram depicts the same for the 168 quasars detected for the first time here. It is apparent that there are very few new detections above 100 mJy.

Using the radio flux densities (or upper limits) in conjunction with the redshifts as given by VV, we have calculated a radio luminosity (or upper limit) for each quasar using the equations from Weedman (1986), where we have assumed a radio spectral index of  $-0.5$ , a Hubble constant of  $H_0 = 50 \text{ km s}^{-1} \text{ Mpc}^{-1}$  and  $q_0 = 0.5$ . Furthermore, using the same spectral index we have adjusted the radio luminosity to 8.4 GHz to facilitate comparisons to previously published results (e.g. Hooper *et al.* 1996). In Figures 4 and 5, we show the distribution of  $L_R$  as a function of redshift  $z$  and  $M_B$  (as given in VV with a correction to  $q_0 = 0.5$ ). Using  $10^{32} \text{ ergs/sec/Hz}$  as the division between radio-loud and radio-quiet, it is clear that the NVSS detects most of the radio-loud quasars out to a redshift of 1.5 while missing most of the radio-quiet quasars. Of the 3280 upper limits, 1799 fall above  $10^{32} \text{ ergs/sec/Hz}$ .

It may be more informative to consider the ratio of radio to optical luminosity  $L_R/L_O$  in defining radio loud quasars. In Figures 6 and 7, we plot  $\log(L_R/L_O)$  against  $z$  and  $M_B$ . In this context, the divide between radio-loud and radio-quiet is often taken to be 1.0. There are only 139 upper limits which lie above this divide. Lastly, using 1.0 as the divide between radio-loud and radio-quiet, we calculate  $F_{RLQ}$  as a function of  $M_B$  and  $z$  (see Figures 8 and 9) where we have not included upper limits above 1.0 in the calculation. The dependence of  $F_{RLQ}$  on  $M_B$  is minimal, remaining nearly constant at  $\sim 0.16$  between  $M_B$  of  $-23$  to  $-29$ . At  $M_B = -30$ ,  $F_{RLQ}$  may decline to below 0.10. The case is quite different for the dependence on redshift.  $F_{RLQ}$  rises dramatically between  $z=0$  and  $z=0.5$  from an initial value of 0.05 up to 0.25. Beyond  $z=1.0$ ,  $F_{RLQ}$  appears to slowly decrease to 0.12 at  $z=2$  and then remain approximately constant out to  $z=4$ . These results are similar to the

$z$  dependence reported by Hooper *et al.* (1995,1996) on a much smaller sample from the LBQS.

#### 4. Discussion

Considerable effort has been expended over the past several decades to understand the underlying difference between radio-loud and radio-quiet quasars. These studies have recently focussed on two specific questions; namely, do the radio properties of quasars evolve with time and do they correlate with optical luminosity? Unfortunately the answers to these questions seem to differ from quasar sample to quasar sample. For example, Hooper *et al.* (1996) found that  $F_{\text{RLQ}}$  was nearly constant at 0.10 over a large range of absolute B magnitude. In contrast they pointed out that a similar analysis of the Palomar Green sample (Schmidt and Green 1983; Kellermann *et al.* 1989) revealed strong variations in  $F_{\text{RLQ}}$  with absolute B magnitude. Hooper *et al.* (1996) were at a loss to explain the difference.

Our comparison between the VV catalog and the NVSS has yielded radio data on a quasar sample which is an order of magnitude larger than previous samples. In general, the radio properties of this sample are very similar to those of the LBQS. In particular,  $F_{\text{RLQ}}$  for this new large sample is also largely independent of absolute B magnitude as shown in Figure 8. Likewise, in agreement with the LBQS sample, we see a peak in  $F_{\text{RLQ}}$  between  $z$  of 0.5 to 1.0. However, with this larger sample, we can study the dependence on  $z$  with much higher resolution and as a result, find a significantly stronger dependence on  $z$ . In particular, we find that  $F_{\text{RLQ}}$  is a factor of five lower today than it was at  $z=0.5$ . While there has been considerable discussion in the literature on the differential evolution of radio-loud quasars at very high redshifts, our results suggest that differential evolution of radio-loud quasars has been most important over the last several billion years.

As we noted at the outset of this paper, to obtain a larger sample we sacrificed the

uniformity of the sample. It is possible that the extreme differential evolution we observe between  $z$  of 0 and 0.5 is a consequence of various selection effects. For example, the nearby quasar population has a higher proportion of low luminosity objects. This in principle could bias the dependence of radio-loud fraction on redshift. However we do not see a dependence of radio-loud fraction on optical luminosity. While we cannot rule out some unforeseen bias, we are encouraged that the LBQS sample also shows a peak at  $z$  of 1, albeit with less statistical significance and resolution.

This type of study and the conclusions drawn from it certainly should be used carefully in light of the heterogenous nature of the quasar sample. This is particularly true in regions of parameter space where the sample is very sparse, such as at very high redshift or luminosity. However, selection effects are probably less important at lower redshifts where quasars are well-sampled and easier to detect. In particular, it is hard to see how radio-loud quasars could be selected against at low redshift, so we think it very likely that this absence at low redshift is a real effect.

### **Acknowledgements**

The authors thank Chris Impey for many useful comments. This work was supported in part under the auspices of the Department of Energy by Lawrence Livermore National Laboratory under contract W-7405-ENG-48 and by the Institute of Geophysics and Planetary Physics.

## REFERENCES

- Condon, J.J., Cotton, W.D., Greisen, E.W., Yin, Q.F., Perley, R.A., and Broderick, J.J.  
1994 preprint.
- Hewett, P.C., Foltz, C.B., and Chaffee, F.H., 1995, AJ , 109, 1498
- Hooper, E.J., Impey, C.D., Foltz, C.B., and Hewett, P.C., 1995, ApJ, 445, 62
- Hooper, E.J., Impey, C.D., Foltz, C.B., and Hewett, P.C., 1996, ApJ, 473, 746
- Kellermann, K.I., Sramek, R., Schmidt, M., Shaffer, D.B., and Green, R., 1989, AJ, 98,  
1195.
- Schmidt, M. and Green, R.F., 1983, ApJ, 269, 352
- Veron-Cetty, M.-P and Veron, P., (VV), 1996, ESO Scientific Report No.X.
- Weedman, D.W. , Quasar Astronomy, Cambridge University Press, 1986, pages 62-64



### Figure Captions

Fig. 1.— Location of VV quasars falling within the area covered by the NVSS. Right ascension increases from left to right in the figure starting at 0 hours. Declination varies in degrees from  $-90$  to  $+90$  as shown.

Fig. 2.— A histogram of the separations between VV quasars and NVSS radio sources as well as an estimate of the chance coincidence rate using a false quasar catalog generated by shifting VV positions by 1 degree.

Fig. 3.— A histogram of radio flux densities for the 799 detections of VV quasars. The shaded histogram is the subset of new detections.

Fig. 4.— The distribution of radio luminosity corrected to 8.4 GHz vs. redshift. The triangles are positive detections and the dots are upper limits.

Fig. 5.— The distribution of radio luminosity at 8.4 GHz versus absolute B magnitude. The triangles are positive detections and the dots are upper limits.

Fig. 6.— Distribution of ratio of radio to optical luminosity versus redshift. Upper limits are dots and positive detections are triangles.

Fig. 7.— Distribution of ratio of radio to optical luminosity versus absolute B magnitude. Upper limits are dots and positive detections are triangles.

Fig. 8.— Radio loud fraction as function of absolute B magnitude. Error bars are plus or minus one standard deviation. The error is for the standard deviation of a random binomial distribution in the radio loud fraction.

Fig. 9.— Radio loud fraction as function of redshift. The error is computed the same way as in the previous plot.

Table 1. New Quasar Radio Detections

R.A.(2000)	Dec.(2000)	$z$	$S_{1400}$ (mJY)	$M_B$	$\log L_{8400}$
00 00 41.9	-02 29 23	1.07	7.2	-26.3	32.1
00 01 50.0	-01 59 40	2.82	37.1	-27.4	33.7
00 05 07.0	-01 32 46	1.71	73.1	-25.9	33.5
00 07 27.1	02 41 12	0.30	8.0	-23.5	31.1
00 27 17.3	00 37 23	1.23	4.6	-26.1	32.1
00 31 36.5	-01 36 22	2.38	16.6	-26.7	33.2
00 39 42.4	-39 29 14	1.46	4.6	-25.9	32.2
00 39 42.5	-35 28 02	0.84	92.2	-25.2	33.0
00 41 50.6	-38 20 09	1.74	71.2	-24.8	33.5
00 41 59.9	-39 21 47	1.85	4.9	-26.7	32.4
00 42 16.5	-02 54 22	2.74	31.6	-27.3	33.6
00 42 40.7	-33 39 20	2.06	6.4	-25.8	32.6
00 42 59.9	-30 07 42	0.61	39.1	-24.7	32.4
00 43 22.4	-26 39 05	1.00	80.1	-26.4	33.1
00 43 51.3	-28 27 41	0.84	55.2	-25.1	32.8
00 48 10.3	-40 05 34	1.64	8.1	-26.2	32.6
00 49 40.8	-26 32 59	3.16	39.0	-25.9	33.8
00 50 40.9	-25 41 24	0.78	43.7	-24.5	32.7
00 51 30.4	00 41 50	1.19	16.3	-25.8	32.6
00 51 53.6	-27 56 18	1.15	6.8	-23.8	32.2
00 52 05.5	00 35 38	0.40	135.3	-25.3	32.6
00 52 45.4	-26 24 23	2.22	5.6	-25.0	32.6
00 52 52.4	-28 25 55	1.65	226.6	-26.1	34.0
00 54 04.0	-27 10 10	0.69	7.0	-23.9	31.8
00 54 24.9	-25 24 00	1.95	112.5	-24.7	33.8

Table 1—Continued

R.A.(2000)	Dec.(2000)	$z$	$S_{1400}$ (mJY)	$M_B$	$\log L_{8400}$
00 54 41.2	00 01 10	0.65	4.4	-25.0	31.5
00 54 45.4	-38 44 15	3.18	29.0	-26.9	33.7
00 55 19.8	-29 59 33	2.10	40.1	-25.3	33.5
00 55 35.1	01 40 35	0.44	26.8	-24.2	32.0
00 55 42.8	-27 23 19	1.54	9.9	-25.1	32.6
00 56 04.3	-26 52 57	1.04	21.7	-25.2	32.6
00 58 01.8	15 53 15	1.26	6.1	-26.3	32.2
00 58 41.2	-39 08 42	1.41	8.6	-26.8	32.5
00 59 17.6	01 42 06	3.15	6.5	-27.8	33.0
00 59 58.1	-39 35 56	2.04	10.2	-25.7	32.8
01 00 12.3	-27 08 53	3.52	210.9	-27.4	34.6
01 00 59.8	-28 51 15	0.87	8.8	-25.4	32.1
01 02 00.6	-30 18 27	1.03	78.7	-26.6	33.2
01 02 59.8	-27 23 43	1.42	3.8	-25.2	32.1
01 03 29.4	00 40 54	1.44	117.9	-25.5	33.6
01 04 03.5	-29 43 53	1.32	13.1	-24.1	32.6
01 09 28.8	-34 05 18	0.83	26.8	-23.3	32.5
01 09 52.0	-35 25 56	2.19	2.8	-25.0	32.3
01 11 08.1	-35 35 17	2.36	15.0	-26.4	33.1
01 11 19.5	-33 08 22	2.31	3.1	-26.0	32.4
01 15 47.7	-33 07 15	1.91	80.1	-24.3	33.7
01 16 36.9	-34 57 01	1.96	107.5	-25.7	33.8
01 22 04.4	-33 10 12	1.11	17.9	-26.7	32.6
01 26 55.8	-32 08 10	2.20	4.5	-27.5	32.5
01 27 44.0	-34 57 54	2.16	18.8	-26.5	33.2

Table 1—Continued

R.A.(2000)	Dec.(2000)	$z$	$S_{1400}$ (mJY)	$M_B$	$\log L_{8400}$
01 34 05.1	-39 32 15	1.89	12.1	-24.8	32.8
01 34 38.6	-19 32 07	3.13	47.4	-28.4	33.9
01 35 05.7	-07 20 29	1.64	6.8	-26.1	32.5
01 35 35.7	-38 54 25	2.08	182.0	-25.3	34.1
01 35 55.5	00 39 24	1.46	4.7	-24.2	32.2
01 42 54.7	-30 23 45	3.12	5.0	-28.4	32.9
01 42 54.8	-38 56 46	2.21	4.0	-25.6	32.5
01 52 27.3	-20 01 07	2.15	26.9	-27.7	33.3
01 52 59.1	-01 29 40	2.02	47.7	-26.8	33.5
01 57 08.6	01 38 24	2.13	4.8	-26.7	32.5
01 59 21.0	19 00 32	2.61	21.9	-26.1	33.4
02 16 12.3	-01 05 19	2.15	144.0	-27.0	34.0
02 42 05.2	-23 44 53	2.63	29.5	-26.4	33.5
02 42 40.3	00 57 27	0.57	8.3	-25.8	31.7
02 44 50.5	-22 16 01	2.20	24.0	-24.9	33.3
02 45 47.8	-31 37 25	1.88	13.6	-26.3	32.9
02 47 39.1	-00 52 22	2.12	7.9	-25.0	32.8
02 48 06.6	-29 36 36	1.86	3.5	-25.3	32.3
02 50 48.6	00 02 08	0.77	112.7	-24.1	33.1
02 51 46.8	15 50 13	0.49	30.4	-23.1	32.1
02 51 56.2	00 57 06	0.47	7.5	-23.4	31.5
02 56 58.5	00 54 47	1.11	13.2	-24.7	32.4
03 00 29.8	02 40 50	0.12	6.8	-23.0	30.2
03 01 38.2	01 38 17	1.58	8.1	-25.4	32.5
03 05 48.9	-02 40 13	1.27	18.6	-25.6	32.7

Table 1—Continued

R.A.(2000)	Dec.(2000)	$z$	$S_{1400}$ (mJY)	$M_B$	$\log L_{8400}$
03 10 02.0	-37 23 38	0.40	15.5	-24.1	31.6
03 11 39.8	-40 08 42	1.73	9.5	-26.1	32.7
03 16 31.3	01 37 30	0.96	11.5	-24.7	32.3
04 07 28.8	17 50 52	1.71	551.6	-25.4	34.4
04 22 41.8	00 30 20	2.92	20.6	-27.2	33.4
04 29 35.5	-22 41 03	0.27	15.8	-24.1	31.3
04 38 48.1	-36 35 09	0.38	10.6	-24.2	31.4
04 41 22.6	-27 08 20	0.08	34.8	-23.0	30.6
04 43 14.3	-36 46 24	0.68	4.7	-25.6	31.6
04 44 15.2	-30 04 52	2.40	10.1	-27.4	33.0
04 49 21.1	07 29 10	1.46	61.8	-27.5	33.3
04 52 30.1	-29 53 35	0.29	10.0	-25.1	31.2
05 04 55.3	-27 23 11	1.14	183.4	-26.4	33.6
05 58 13.5	-36 19 48	2.22	3.1	-27.0	32.4
06 06 07.2	-34 47 40	2.28	280.4	-26.5	34.4
07 07 13.2	64 35 59	0.08	3.2	-23.1	29.5
07 51 00.7	03 20 41	0.10	12.0	-23.6	30.3
07 58 19.8	42 19 35	0.21	4.0	-24.1	30.5
08 15 20.6	27 36 18	0.91	6.0	-27.4	31.9
08 36 58.9	44 26 02	0.25	7.9	-25.3	30.9
08 38 40.5	47 34 10	0.70	29.6	-23.7	32.4
08 41 18.0	35 44 38	1.77	6.7	-28.7	32.5
08 42 15.2	45 25 44	1.41	75.4	-26.9	33.4
08 47 56.4	31 47 58	1.83	29.0	-26.8	33.2
08 48 47.8	14 20 56	1.69	44.3	-26.5	33.3

Table 1—Continued

R.A.(2000)	Dec.(2000)	$z$	$S_{1400}$ (mJY)	$M_B$	$\log L_{8400}$
08 55 16.1	56 16 56	0.44	5.6	-23.3	31.3
08 56 58.8	51 20 45	2.31	8.6	-25.8	32.9
08 57 06.3	19 08 54	0.33	5.2	-23.8	31.0
09 06 03.6	19 41 44	1.21	17.4	-27.2	32.6
09 28 37.9	60 25 21	0.30	67.8	-23.1	32.0
09 29 58.4	-26 00 31	2.15	2.8	-27.1	32.3
09 32 35.0	21 58 30	2.31	5.9	-25.4	32.7
09 38 57.2	42 48 29	2.04	6.5	-26.2	32.6
09 41 28.8	44 47 43	0.80	69.3	-24.6	32.9
09 47 04.5	47 21 43	0.54	4.0	-24.2	31.3
09 47 56.0	53 50 01	0.49	23.1	-25.2	32.0
09 48 35.9	43 23 02	1.89	2.8	-26.7	32.2
09 52 27.2	50 48 51	1.55	72.3	-26.7	33.5
09 55 38.0	33 35 04	2.50	34.1	-28.5	33.5
10 02 54.6	32 40 39	0.83	11.5	-26.6	32.1
10 17 03.4	59 24 29	0.85	340.5	-25.9	33.6
10 28 09.6	-26 44 18	2.90	933.8	-28.3	35.1
10 38 08.1	47 31 36	2.96	8.6	-25.7	33.1
10 53 33.4	-27 39 07	0.16	12.9	-23.8	30.8
11 03 25.3	-26 45 15	2.15	15.8	-28.9	33.1
11 22 41.5	30 35 35	1.81	10.4	-27.7	32.7
11 27 36.4	26 54 50	0.38	3.2	-24.7	30.9
11 30 04.8	41 16 19	0.72	3.4	-26.0	31.5
11 33 14.8	28 12 00	0.51	12.9	-24.6	31.8
11 41 16.1	21 56 22	0.06	6.1	-23.0	29.6

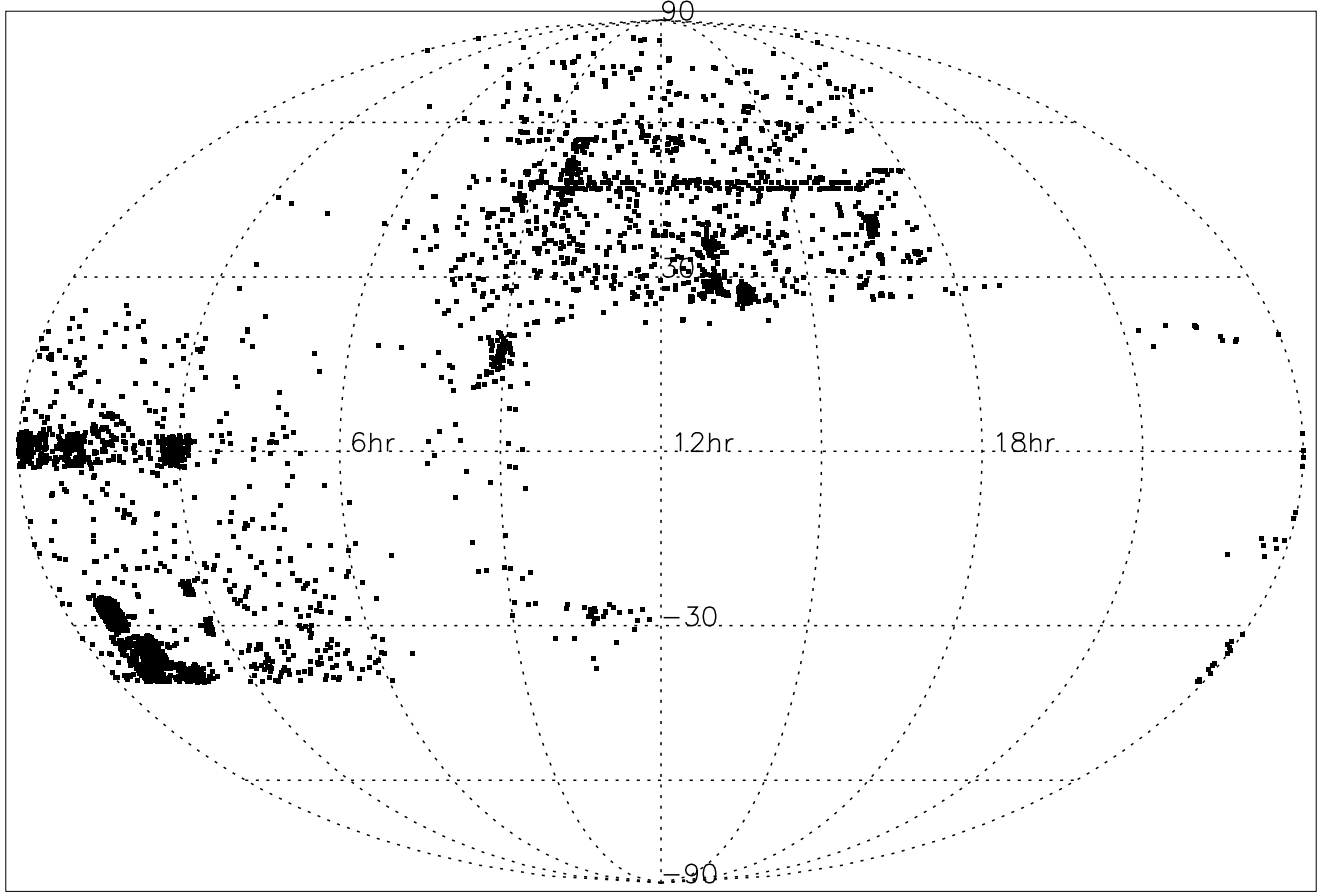
Table 1—Continued

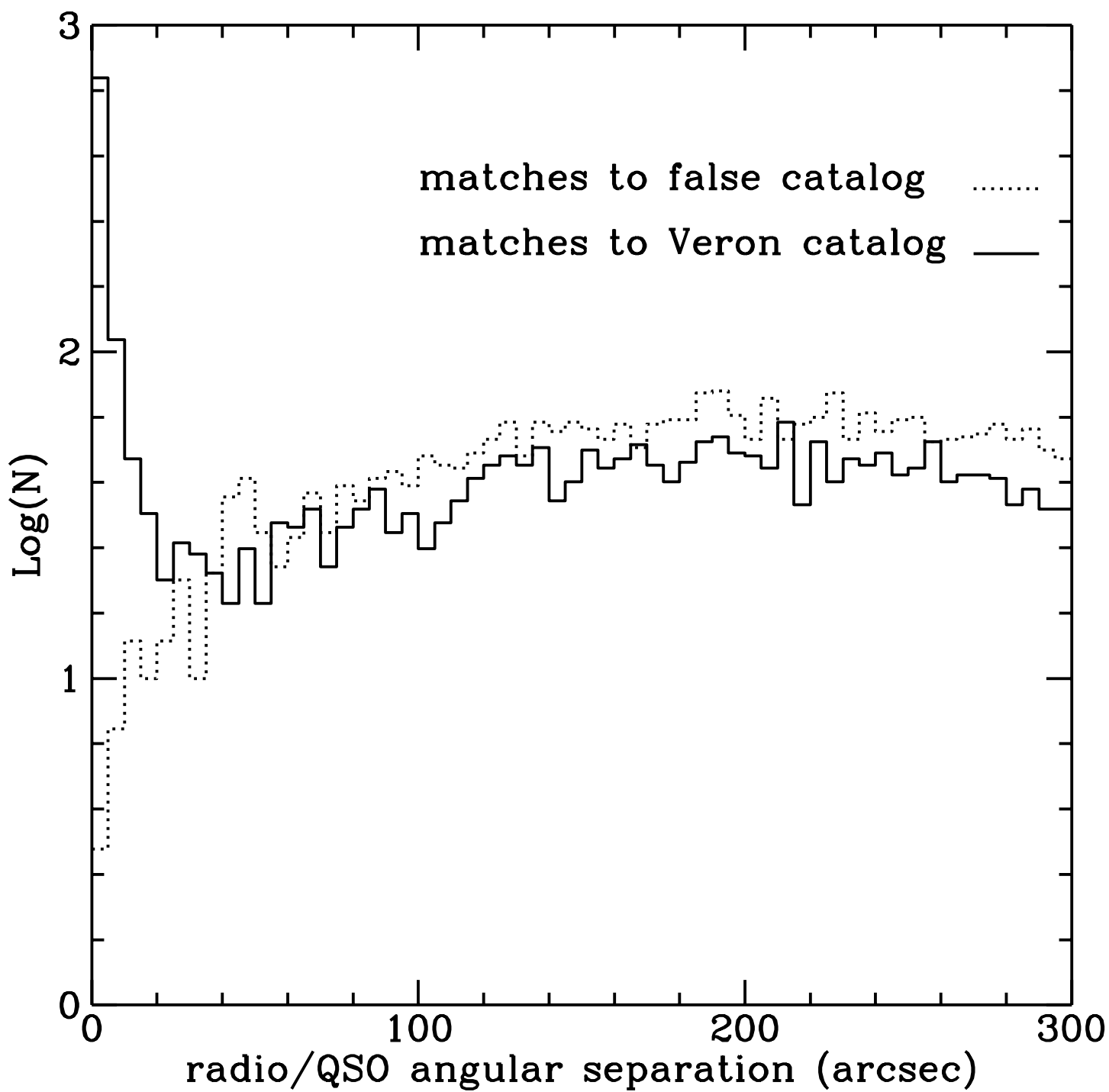
R.A.(2000)	Dec.(2000)	$z$	$S_{1400}$ (mJY)	$M_B$	$\log L_{8400}$
11 48 00.0	26 35 44	0.87	351.4	-25.3	33.7
11 48 18.8	31 54 11	0.55	94.7	-25.0	32.7
11 52 27.5	32 09 59	0.37	41.7	-23.6	32.0
11 57 34.7	73 10 37	0.51	9.5	-25.7	31.6
12 02 43.3	37 35 50	0.50	16.7	-24.2	31.9
12 12 09.4	46 23 46	2.29	4.8	-25.6	32.6
12 17 21.3	30 56 31	0.31	8.4	-24.2	31.1
12 17 36.6	51 55 11	2.23	85.2	-28.6	33.8
12 19 43.6	54 08 35	1.66	45.0	-26.1	33.3
12 33 22.9	47 38 43	2.23	24.3	-25.0	33.3
12 37 14.4	26 19 00	2.20	3.9	-23.4	32.5
13 10 21.1	47 34 03	3.58	9.2	-24.2	33.3
13 11 04.3	29 26 13	1.82	10.4	-27.4	32.8
13 12 11.0	48 09 25	0.72	45.0	-25.4	32.6
13 18 01.9	47 06 27	2.59	2.8	-27.3	32.5
13 18 50.9	26 41 42	1.91	23.1	-23.8	33.1
13 19 13.8	26 47 54	2.26	8.2	-25.1	32.8
13 22 50.7	47 39 37	1.11	8.1	-25.0	32.2
13 36 02.8	27 27 47	1.12	75.5	-24.5	33.2
13 42 08.3	27 09 23	1.19	270.8	-25.0	33.8
13 44 25.6	26 14 10	1.18	11.2	-24.5	32.4
13 45 43.8	26 25 07	2.03	9.5	-24.6	32.8
13 45 44.5	26 25 06	2.03	9.5	-25.0	32.8
14 23 14.3	50 55 39	0.28	180.5	-24.3	32.4
14 43 00.6	52 01 37	1.57	2550.8	-24.5	35.0

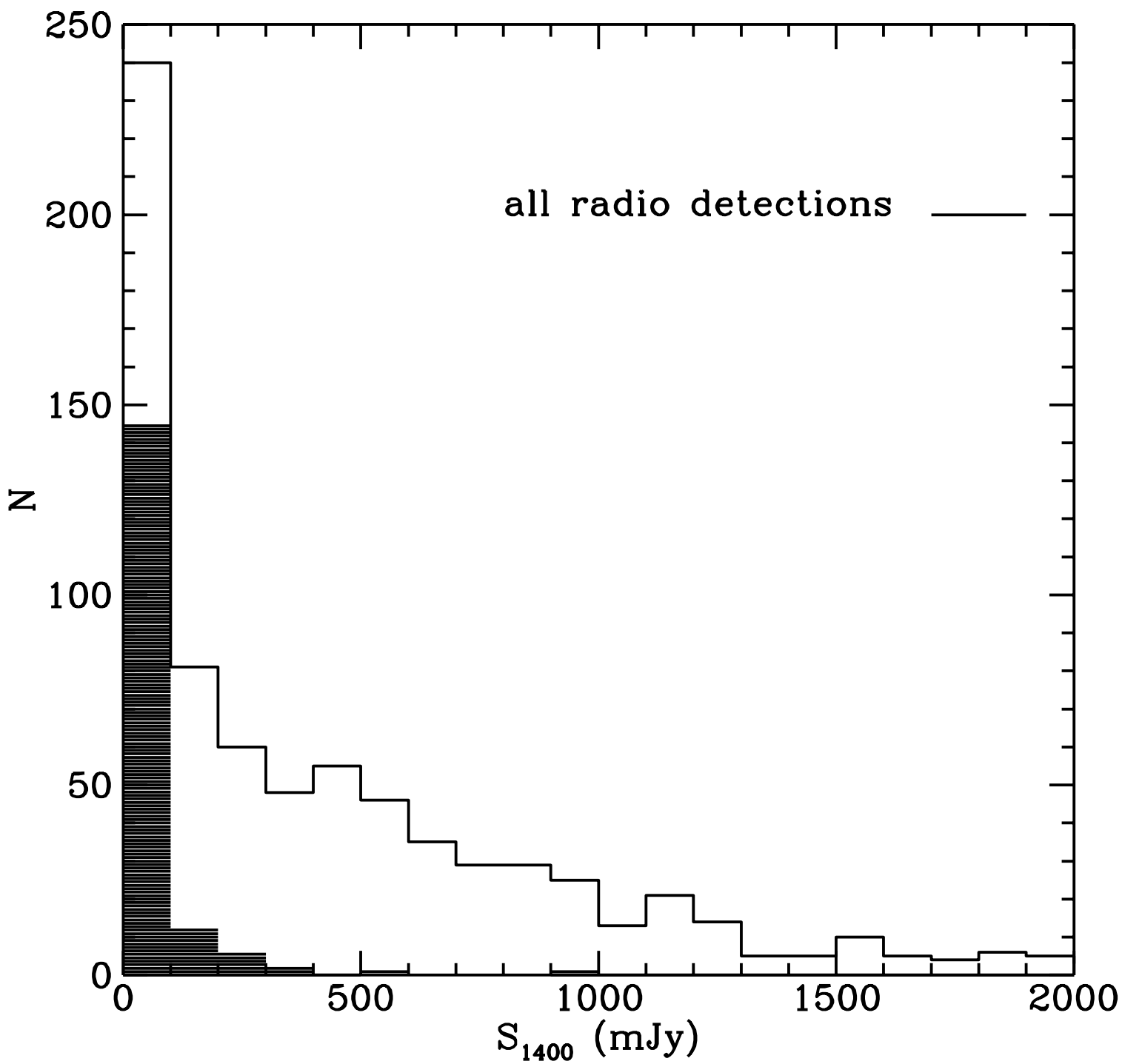
Table 1—Continued

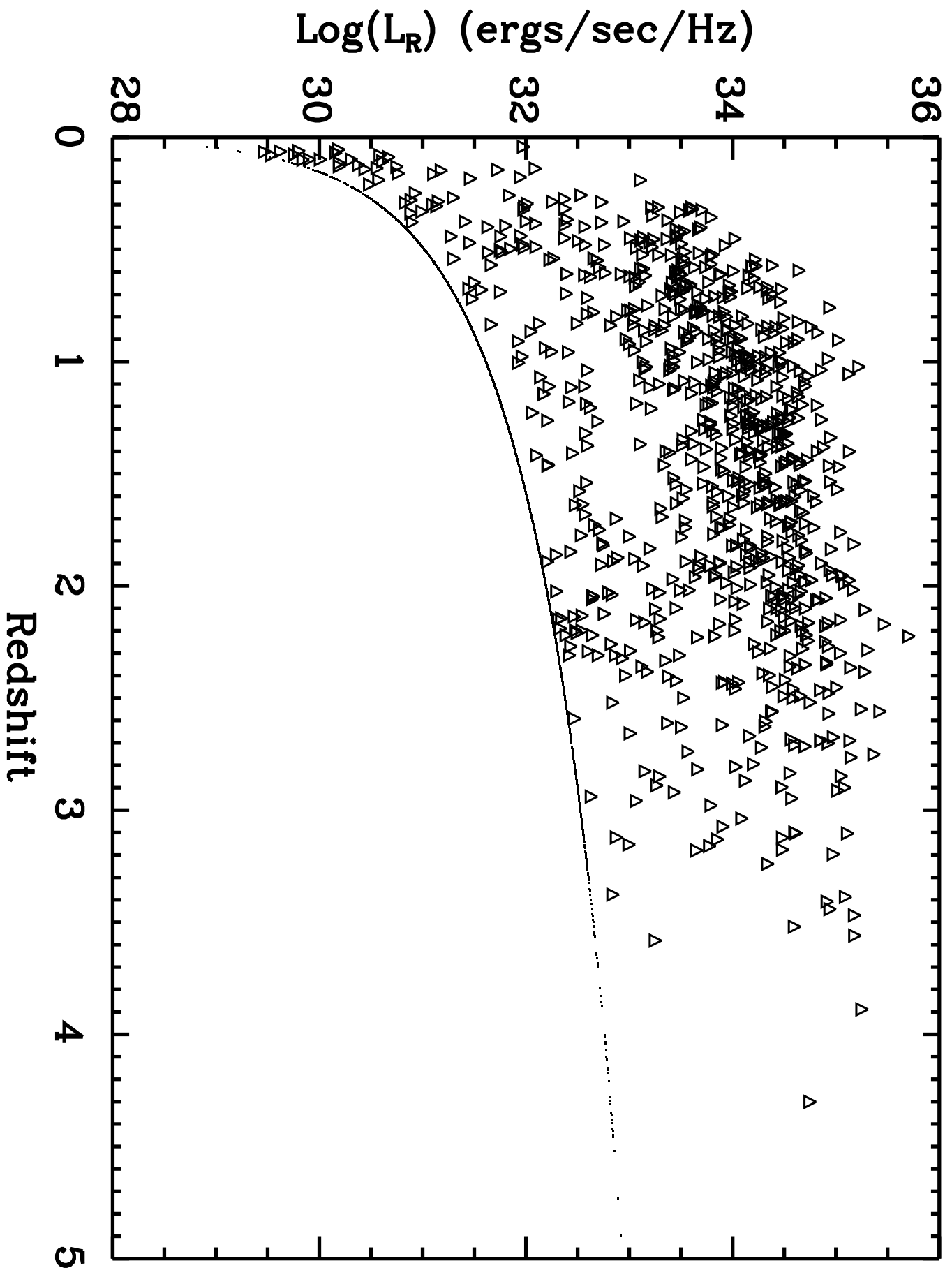
R.A.(2000)	Dec.(2000)	$z$	$S_{1400}(\text{mJY})$	$M_B$	$\log L_{8400}$
14 49 20.7	42 21 02	0.18	160.1	-23.1	31.9
14 50 05.0	46 35 19	0.29	4.6	-23.1	30.8
15 19 07.5	52 06 05	0.14	11.1	-23.3	30.6
15 20 43.6	47 32 49	2.81	87.5	-26.2	34.0
15 29 07.4	56 16 07	0.10	6.0	-23.0	30.0
15 29 17.6	47 38 38	3.07	55.5	-26.2	33.9
15 30 45.8	38 39 53	2.02	3.0	-28.0	32.3
15 34 57.2	58 39 24	1.90	129.5	-25.9	33.9
15 40 58.6	47 38 28	2.56	230.0	-26.0	34.4
15 56 10.6	37 40 40	2.66	9.2	-26.9	33.0
16 25 48.8	26 46 59	2.52	6.9	-29.6	32.8
16 30 20.8	37 56 56	0.39	23.8	-24.8	31.8
16 32 49.6	37 16 31	2.94	3.2	-27.6	32.6
16 45 01.8	39 25 48	2.15	3.0	-26.0	32.3
16 50 05.5	41 40 33	0.59	234.7	-25.2	33.1
16 56 41.1	59 15 39	0.50	13.0	-23.7	31.8
17 51 05.5	26 59 02	0.14	146.4	-24.5	31.7
18 30 23.3	73 13 10	0.12	9.1	-23.8	30.4



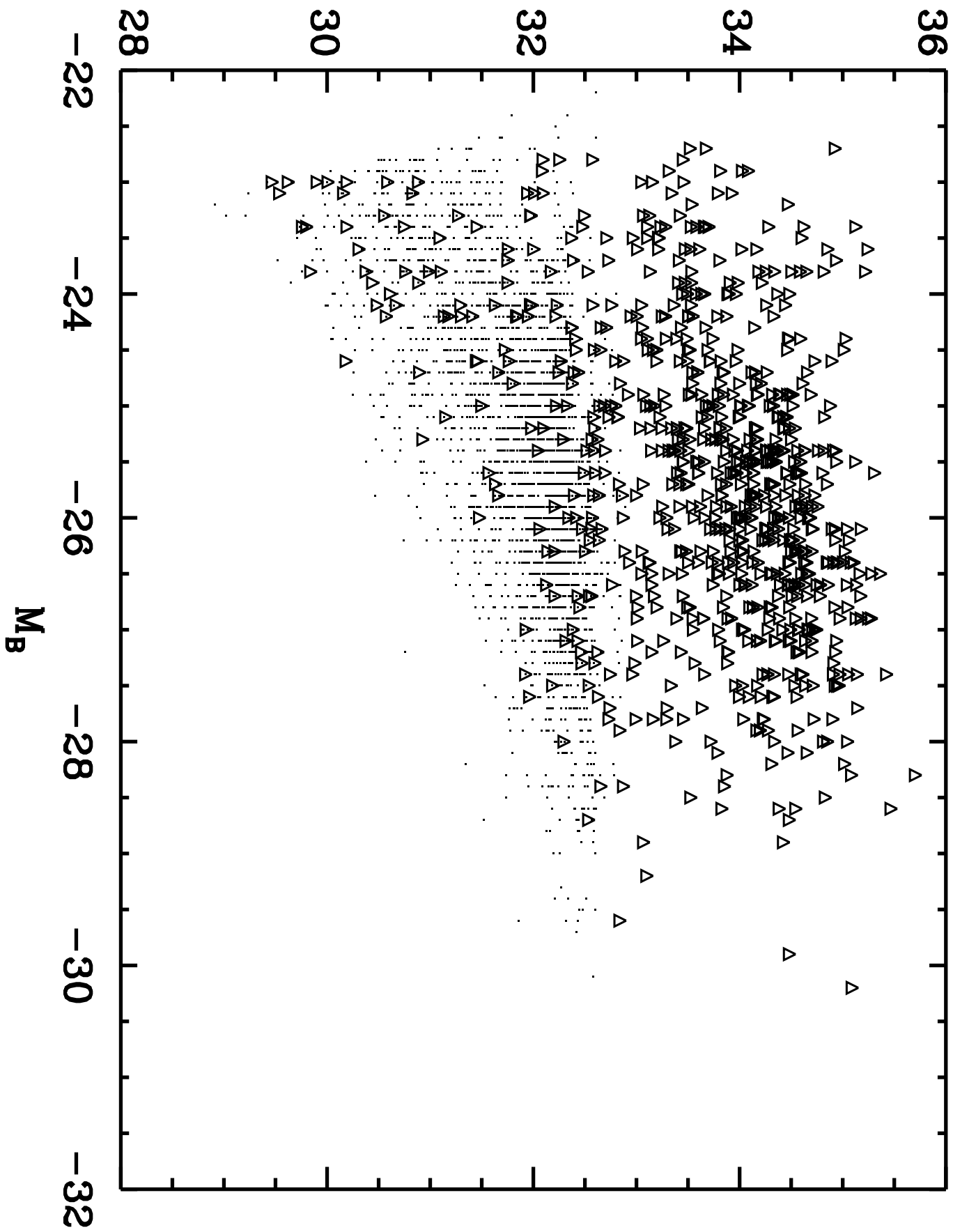


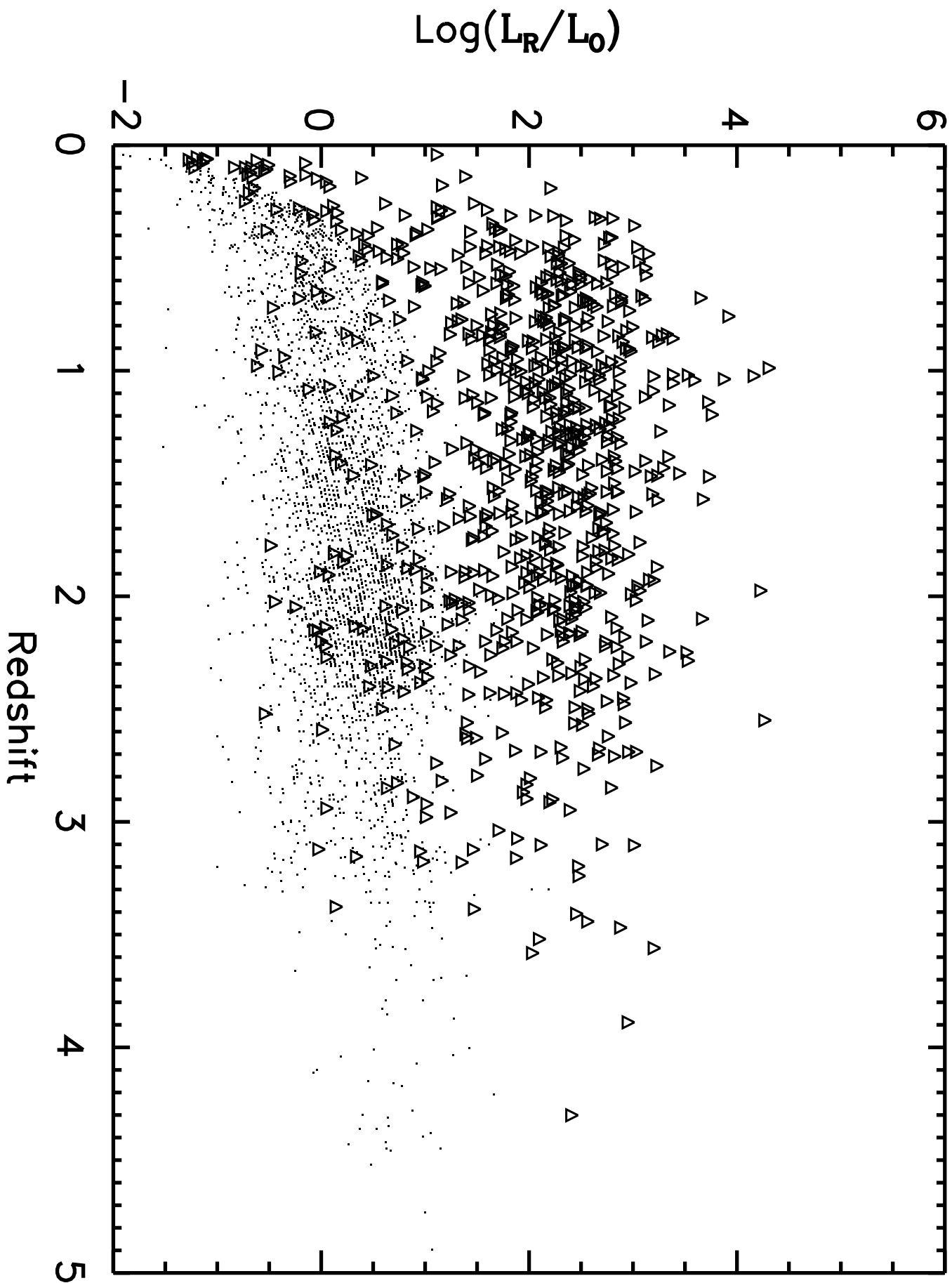




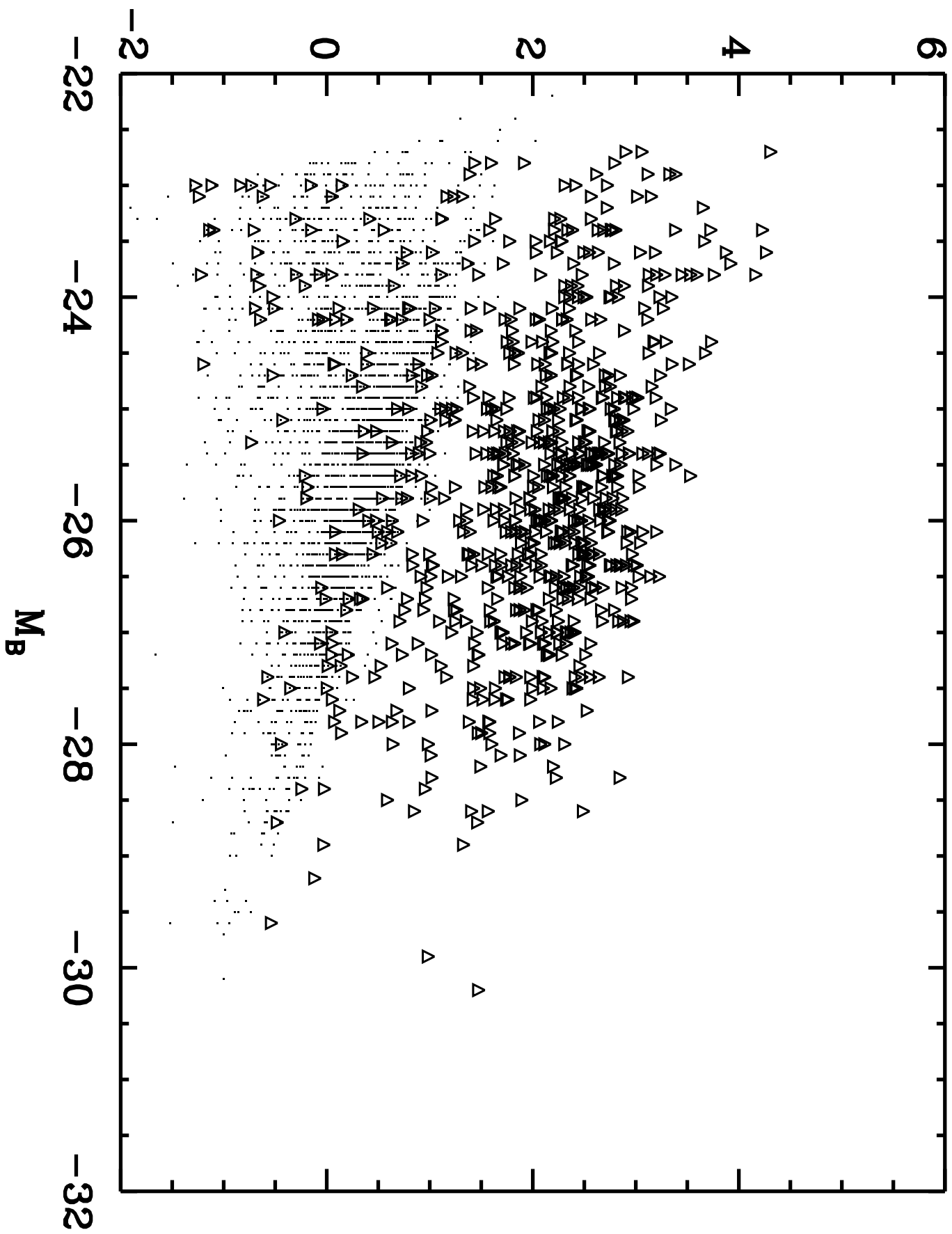


$\text{Log}(L_R)$  (ergs/sec/Hz)





$\text{Log}(L_R/L_0)$



# Radio loud fraction

